

# Supernovae at the Highest Angular Resolution<sup>1</sup>

Schuyler D. Van Dyk

IPAC/Caltech, Mailcode 100-22, Pasadena CA 91125

K.W. Weiler

Naval Research Laboratory, Code 7214, Washington, DC 20375-5320

R.A. Sramek

National Radio Astronomy Observatory, P.O. Box 0, Socorro, NM 87801

N. Panagia

Space Telescope Science Institute, 3700 San Martin Drive, Baltimore, MD 21218

C.K. Lacey

Naval Research Laboratory, Code 7214, Washington, DC 20375-5320

M.J. Montes

Naval Research Laboratory, Code 7214, Washington, DC 20375-5320

J. Marcaide

Departamento de Astronomia, Universitat de Valencia, 46100 Burjassot, Spain

W.H.G. Lewin

Massachusetts Institute of Technology, Department of Physics, 37-627, Cambridge, MA  
02139

---

<sup>1</sup>Based in part on observations made with the NASA/ESA *Hubble Space Telescope*, obtained from the data archive of the Space Telescope Science Institute, which is operated by the Association of Universities for Research in Astronomy, Inc., under NASA contract NAS 5-26555.

Derek Fox

Massachusetts Institute of Technology, Department of Physics, 37-627, Cambridge, MA  
02139

Alexei V. Filippenko

Astronomy Department, University of California, Berkeley, CA 94720-3411

and

Chien Y. Peng

Steward Observatory, Astronomy Department, University of Arizona, Tucson, AZ 85726

Received \_\_\_\_\_; accepted \_\_\_\_\_

To be presented at IAU Symposium 205

## ABSTRACT

The study of supernovae (SNe) and their environments in host galaxies at the highest possible angular resolution in a number of wavelength regimes is providing vital clues to the nature of their progenitor stars. We are observing SNe in the radio using the VLA and VLBI and in the X-rays using *Chandra*, to probe the density and structure of the circumstellar environment and, by inference, the evolution of the presupernova stellar wind, revealing the last stages of stellar evolution of the SN progenitor prior to explosion. We will discuss some examples, including exciting recent combined radio/X-ray results for SNe 1999em in NGC 1637 and 1998S in NGC 3877. We are also studying SNe and their local stellar and gaseous environments with the subarcsecond resolution of *HST*. The *HST* resolution has allowed us to detect late-time optical emission from SNe. For the first time, we can also resolve individual stars in, and to derive detailed color-magnitude diagrams for, several environments. As a result, we are able to place rigorous constraints on the masses of the SN progenitors. In particular, we highlight the results for the Type II SNe 1979C in M100 and 1997bs in M66 (for which we may have directly identified the progenitor star).

## 1. Radio Supernovae

The study of supernovae (SNe) which are significant sources of radio emission, known as “radio supernovae” (RSNe), provides unique information on the properties of the progenitor stellar systems and their immediate circumstellar environments. In particular, changes in the density of the presupernova stellar wind established circumstellar material (CSM) alter the intensity of the radio emission and allow us to probe the mass-loss history of the supernova’s progenitor, structures in the CSM, and the nature and evolution of the SN progenitor.

Significant deviation of the radio emission of SNe from standard models has previously been noted and interpreted as due to a complex CSM density structure. SN 1979C has shown a quasi-periodic variation in its radio emission which may be due to modulation of the CSM density by a binary companion. SN 1987A, after an initial, faint radio outburst and rapid decline until 1990 June, is now increasing in radio flux density due to the SN shock starting to impinge on the inner edges of the well known, much higher density central ring. SN 1980K at an age of  $\sim 10$  years has experienced a sharp drop in its radio emission far beyond that expected from models of its previous evolution. More recently, SN 1988Z has also shown a sharp drop in its radio emission similar to that of SN 1980K.

Recent observations of SN 1979C imply that the shock from SN 1979C has entered a new, higher density CSM structure different from the modulated decline previously reported. The radio emission has apparently stopped declining and has been constant, or perhaps increasing, for the past eight years.

We present new radio observations of the supernova SN 1979C made with the VLA at 20, 6, 3.6, and 2 cm from 1991 July to 1998 October, which extend our previously published observations, beginning 8 days after optical maximum in 1979 April and continuing through 1990 December. We find that the radio emission from SN 1979C has stopped declining

in flux density, and has apparently entered a new stage of evolution. The observed “flattening,” or possible brightening, of the radio light curves for SN 1979C is interpreted as due to the SN shock wave entering a denser region of material near the progenitor star and may be indicative of complex structure in the circumstellar medium established by the stellar wind from the red supergiant (RSG) progenitor.

SN 1980K [RA(1950.0)=  $20^{\text{h}}34^{\text{m}}26^{\text{s}}.68 \pm 0^{\text{s}}.01$ ; Dec(1950.0)=  $+59^{\circ}55'56''.5 \pm 0''.2$ ] in NGC 6946 was discovered in 1980 October, and an initial, unsuccessful attempt was made on 1980 November 3 to detect it at 6 cm with the Very Large Array (VLA).<sup>2</sup> However, only 35 days after optical maximum SN 1980K was detected at 6 cm on 1980 December 4 and has been regularly monitored at 20, 6, and occasionally 2 cm since then. Results from 1980 November through 1984 August and results from 1984 November through 1990 December have been previously presented. By 1990 December the flux density had fallen to  $S < 0.3$  mJy at 20 and 6 cm, which made it difficult to observe with the VLA using typical, short “snapshot” observations, and regular monitoring was terminated.

However, optical imaging and spectra taken after 1990 indicated that SN 1980K was still a detectable, albeit relatively constant optical luminosity source, particularly at  $\text{H}\alpha$ . Late-time optical and radio emission are predicted to be correlated, and in several examples are indeed observed to be related. Therefore, deeper and more sensitive VLA observations were made in 1994, 1995, and 1996 at both 20 and 6 cm, to attempt to obtain new measurements of SN 1980K below our previous sensitivity limits. Interestingly, these new data indicate that SN 1980K has, in fact, *not* continued along its previously observed power-law decline, but has dropped sharply in radio flux density in the interval between

---

<sup>2</sup>The VLA is operated by the National Radio Astronomy Observatory (NRAO) of Associated Universities, Inc., under a cooperative agreement with the National Science Foundation.

1990 and 1994. Additionally, recent measurements indicate that SN 1980K has also faded in the optical over the last several years, possibly starting with a 20% decline by 1994. The new radio measurements are presented here, and they indicate a significant change in the evolution of the radio emission of SN 1980K from earlier, model-based expectations.

New observations of SN 1980K made with the VLA at 20 and 6 cm from 1994 April through 1996 October show that the supernova (SN) has undergone a significant change in its radio emission evolution, dropping by a factor of  $\sim 2$  below the flux density  $S \propto t^{-0.73}$  power-law decline with time  $t$  observed earlier. However, although  $S$  at all observed frequencies has decreased significantly, its current spectral index of  $\alpha = -0.42 \pm 0.15$  ( $S \propto \nu^{\alpha}$ ) is consistent with the previous spectral index of  $\alpha = -0.60^{+0.04}_{-0.07}$ .

It is suggested that this decrease in emission may be due to the SN shock entering a new region of the circumstellar material which has a lower density than that expected for a constant speed ( $w$ ), constant mass-loss rate ( $\dot{M}$ ) wind from the progenitor. If such an interpretation is correct, the difference in wind and shock speeds appears to indicate a significant evolution in the mass-loss history of the SN progenitor  $\sim 10^4$  years before explosion, with a change in circumstellar density ( $\propto \dot{M}/w$ ) occurring over a time span of  $\lesssim 4$  kyr. Such features could be explained in terms of a fast “blue-loop” evolutionary phase of a relatively massive pre-SN progenitor star. If so, we may, for the first time, provide a stringent constraint on the mass of the SN progenitor based solely on the SN’s radio emission.

## 2. VLBI Observations

A rarity among supernova, SN 1993J in M81 can be studied with high spatial resolution. Its radio power and distance permit VLBI observations to monitor the expansion

of its angular structure. This radio structure was previously revealed to be shell-like and to be undergoing a self-similar expansion at a constant rate. From VLBI observations at wavelengths of 3.6 and 6 cm in the period 6-42 months after explosion, we have discovered that the expansion is decelerating. Our measurement of this deceleration yields estimates of the density profiles of the supernova ejecta and circumstellar material in standard supernova explosion models.

Supernova SN 1993J in M81, discovered by Francisco Garca of Lugo, Spain, is a Type IIb supernova (SN) whose red giant progenitor probably had a mass of 12–16 Msuns while on the main sequence; at the time of the explosion, 3–5 Msuns likely remained in the He core and 1 Msun in the He/H envelope. The first maximum in the SN optical light curve has been attributed to shock heating of the thin envelope and the second to radioactive decay of  $^{56}\text{Co}$ . Modeling of the X-ray emission also implies an envelope of relatively low mass due to interaction with a binary companion.

The standard circumstellar interaction model, standard model, for radio SNs (Chevalier 1996, and references therein) suggests that the radio emission arises from a shocked region between the SN ejecta and the circumstellar material (CSM) that results from the wind of the SN's progenitor star. More specifically, the SM considers SN ejecta with steep density profiles ( $\rho \propto r^{-n}$ ) shocked by a reverse shock that moves inward from the contact surface and a CSM with density profile  $\rho \propto r^{-s}$  shocked by a forward shock that moves outward from the contact surface ( $s = 2$  corresponds to a steady wind). For  $n \geq 5$ , self-similar solutions are possible: the radii of the discontinuity surface, forward shock, and reverse shock are then related, and all evolve in time with the power law  $R \propto t^m$ , where  $t$  is time after explosion and the deceleration parameter,  $m$ , is  $(n - 3)/(n - s)$ .

SN 1993J is the closest SN that is both young and radio bright and hence offers a unique opportunity for the study of its radio structure and the test of radio SN models.

The radio structure is shell-like. Multiwavelength radio light curves and high-resolution radio images of SN 1993J established the self-similar nature of the expansion.

The technique of VLBI can, in principle, determine  $m$  directly by simply observing the angular growth rate of the supernova.  $m = 1$  is compatible with their results to within their uncertainties. We present VLBI results at a wavelength of 6 and 20 cm, combined with those already published for at 3.6 cm, to estimate the deceleration in the SN expansion and to infer the density profiles of the SN ejecta and CSM.

### 3. Chandra Observations

To date, just 13 SNe have been detected in X-rays in the near aftermath of their explosions. Of these both SN 1998S and SN 1999em were detected with Chandra as a result of our Cycle 1 prompt observations of nearby SNe.

In general, the high X-ray luminosities of these 13 SNe ( $L_x \sim 10^{32}-10^{41}$  erg/s) dominate the total radiative output of the SNe starting at an age of about one year. This soft X-ray emission is most convincingly explained as thermal radiation from the “reverse shock” region that forms with the expanding SN ejecta as it interacts with the dense stellar wind of the progenitor star.

The interaction of a spherically symmetric SN shock and a smooth circumstellar medium (CSM) has been calculated. As the SN “outgoing” shock emerges from the star, its characteristic velocity is  $\sim 10^4$  km/s, and the density distribution in the outer parts of the ejecta can be approximated by a power law in radius,  $\rho \propto r^{-n}$ , where the value of  $n$  ranges from 7 to 20. The outgoing shock then propagates into the CSM, a slow moving wind with a density that decreases with the inverse square of the radius,  $\rho \propto \dot{M}/r^2 v$ , where  $\dot{M}$  is the stellar wind mass-loss rate and  $v$  is the wind velocity. The collision between the

stellar ejecta and the CSM produces a reverse shock that moves into the stellar ejecta (which is expanding at  $10^4$  km/s) at  $10^3$  km/s. The outgoing shock produces a very hot shell while the reverse shock produces a denser, cooler shell with much higher emission measure, from which most of the observable X-ray emission arises. If either the CSM density or  $n$  is high the reverse shock is radiative, resulting in a dense, partly-absorbing shell between the two shocks.

The outgoing shock from the SN explosion generates the relativistic electrons and enhanced magnetic field necessary for synchrotron radio emission. The CSM initially absorbs most of this emission (except when synchrotron self-absorption dominates, as may have been the case in SN 1993J). As the shock passes through the CSM, however, less and less material is left between the shock and the observer; absorption decreases rapidly, and the observed radio flux density rises accordingly. At the same time, emission from the shock region is decreasing slowly as the shock expands, and, when radio absorption has become negligible, the radio light curve follows the decline.

All known radio supernovae appear to share common properties of (i) nonthermal synchrotron emission with a high brightness temperature, (ii) a decrease in absorption with time, resulting in a smooth, rapid turn-on first at shorter wavelengths, and later at longer wavelengths, (iii) a power law decline of the emission flux density with time at each wavelength after maximum flux density is reached at that wavelength, and (iv) a final, asymptotic approach of the spectral index to an optically thin, nonthermal, constant negative value, all consistent with the Chevalier model.

Considerable observational evidence therefore exists for this interaction of SNe with the winds from presupernova mass loss. The signatures of circumstellar interaction in the radio, optical, and X-ray regimes have been found for a number of Type II and Type Ib/c SNe, and correlate well with the X-ray emission. SN 1979C and SN 1980K are two specific

cases of “normal” Type II SNe. The Type IIn subclass has peculiar optical characteristics: narrow H-alpha emission superposed on a broad base; lack of P Cygni absorption-line profiles; a strong blue continuum; and slow evolution. The narrow optical lines are clear evidence for dense circumstellar gas – they probably arise from the reprocessing of the X-ray emission – and are another significant means by which the shock radiatively cools. The best recent examples are SN 1986J, SN 1988Z, SN 1994W, SN 1995N, and SN 1998S. It is possible that SN 1979C possesses, perhaps in a less extreme form, similar characteristics.

Both SN 1999em and SN 1998S are interesting because they span the extremes of mass loss from a progenitor. The continued monitoring of their fluxes and spectral evolution is crucial for determining which of the possible scenarios for X-ray production applies for each SN. In particular, there are strong predictions for the evolution of X-ray flux, column density and temperature for each scenario.

SN 1999em (Type IIP) exploded on 1999 Oct 29 in NGC 1637 at a distance of 7.8 Mpc. ACIS-S3 observations were performed on 1999 Nov 01, Nov 13, Dec 16, and 2000 Feb 07, and the source was detected on all occasions. The unusually low luminosity ( $L_x \sim 2 \times 10^{38}$  erg/s) of the source resulted in 235 total counts and indicates that the progenitor star had a stellar wind with a low mass-loss rate. Somewhat surprisingly, the flux nearly doubled from the third observation to the fourth, and the spectrum continued to soften throughout all the observations, seen in the rapid decline of the hard X-rays. With so few counts, the data do not constrain the column density of the X-ray temperature very well. However, we can construct multicolor X-ray light curves, which provide insight in the evolution of this SN.

SN 1998S (Type IIn) in NGC 3877 exploded on 1999 Mar 03 and was first detected in the radio on 1999 Oct 28. This triggered our ToO criteria, and Chandra first observed it on 2000 Jan 10 and again on Mar 7. Our last observation is scheduled for 2000 July. Each observation yielded ~700 counts with an unabsorbed 0.2–10 keV luminosity of

$L_x = 1 \times 10^{40}$  erg/s, given a distance of 17 Mpc. Our initial spectral analysis indicates that a single-temperature warm plasma can reproduce the possible emission features around 1 keV and 1.5 keV, but does not give an acceptable fit to the whole spectrum. Our analysis is not yet complete, and we plan to perform the type of analysis done with the ASCA data from SN 1993J, in which the usual 3 keV thermal bremsstrahlung emission from the reverse shock was combined with a hotter component, presumably due to the outgoing shock. In that case, a measurement of the difference in absorbing columns to the cool and hot components allowed a measurement of the thickness of the reverse shock region.

#### 4. HST Observations

The locations of supernovae in the local stellar and gaseous environment in galaxies contain important clues to their progenitor stars. Access to this information, however, has been hampered by the limited resolution achieved by ground-based observations. High spatial resolution *Hubble Space Telescope* (*HST*) images of galaxy fields in which supernovae had been observed can improve the situation considerably. We have examined the immediate environments of several supernovae using archival post-refurbishment *HST* images. Although our analysis is limited due to signal-to-noise ratio and filter bandpass considerations, the images allow us for the first time to resolve individual stars in, and to derive detailed color-magnitude diagrams for, several environments. We are able to place more rigorous constraints on the masses of these supernovae. A search was made for other old SNe in the archival images, and for the progenitor of the Type II<sub>n</sub> SN 1997bs in presupernova images of their host galaxies.

The locations of supernovae in the local stellar and gaseous environment in galaxies contain important clues to their progenitor stars. As part of a program to study the environments of supernovae using *Hubble Space Telescope* (*HST*) imaging data, we have

examined the environment of the Type II-L SN 1979C in NGC 4321 (M100). We place rigorous constraints on the mass of the SN progenitor, based on photometry of the stellar populations in its environment. The progenitor may have had an initial mass  $M \approx 17\text{--}18 (\pm 3)M_{\odot}$ . Moreover, 17 years after explosion we have recovered and measured the brightness of SN 1979C in several bands, e.g.,  $m = 23.37$  in F439W ( $\sim B$ ; for comparison,  $m_B(\text{max}) = 11.6$ ).

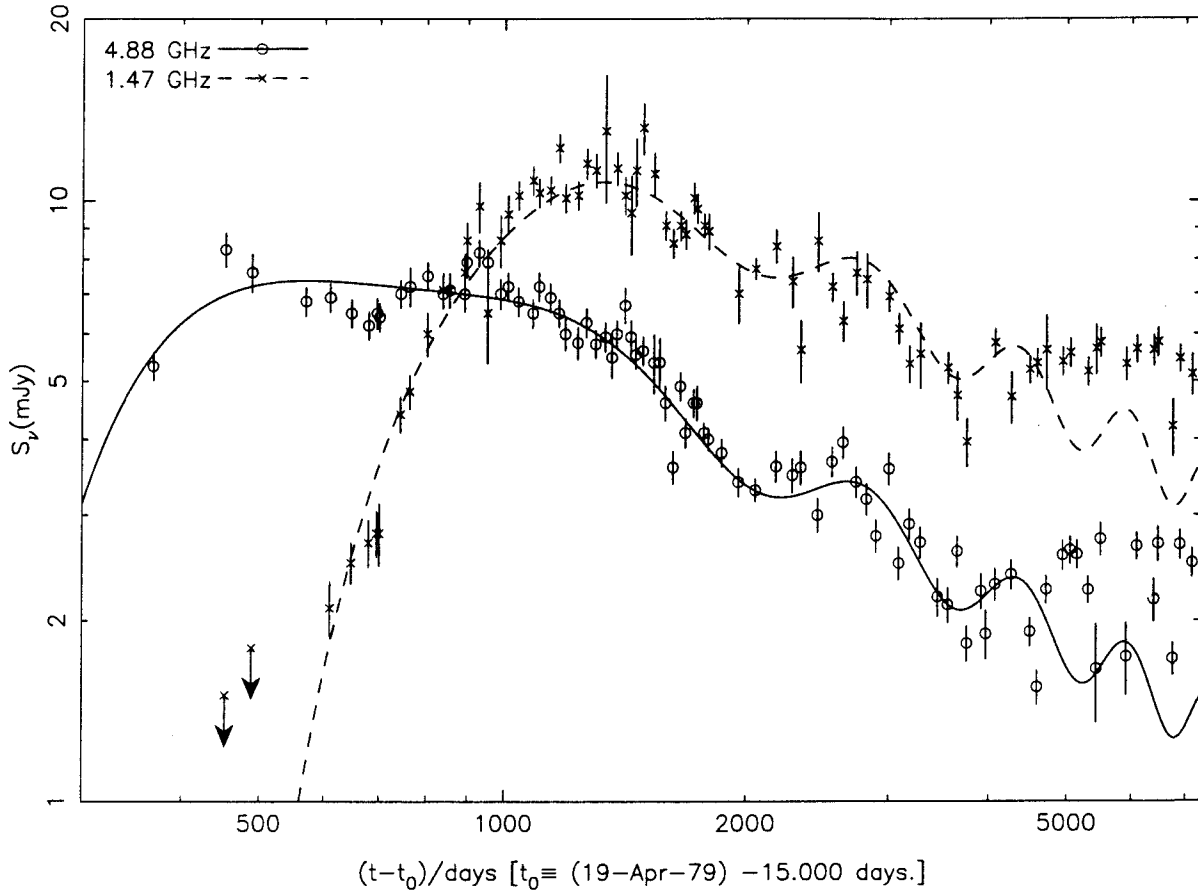


Fig. 1.— Radio “light curves” for SN 1979C in NGC 4321 (M100) at wavelengths 20 cm (*crosses*) and 6 cm (*open circles*). (Since there are only two new measurements available at 3.6 and 2 cm, they are not plotted here. However, they are shown as confirming the nonthermal nature of the spectrum.) The data represents about 18 years of observations for this object, including the new observations presented in this paper and previous observations. The curves represent the best-fit model light curves at 6 cm (*solid*), and 20 cm (*dashed*), including the quasi-periodic, or sinusoidal, term. The best-fit parameters were determined using only data through 1990 December (day  $\sim 4,300$ ).

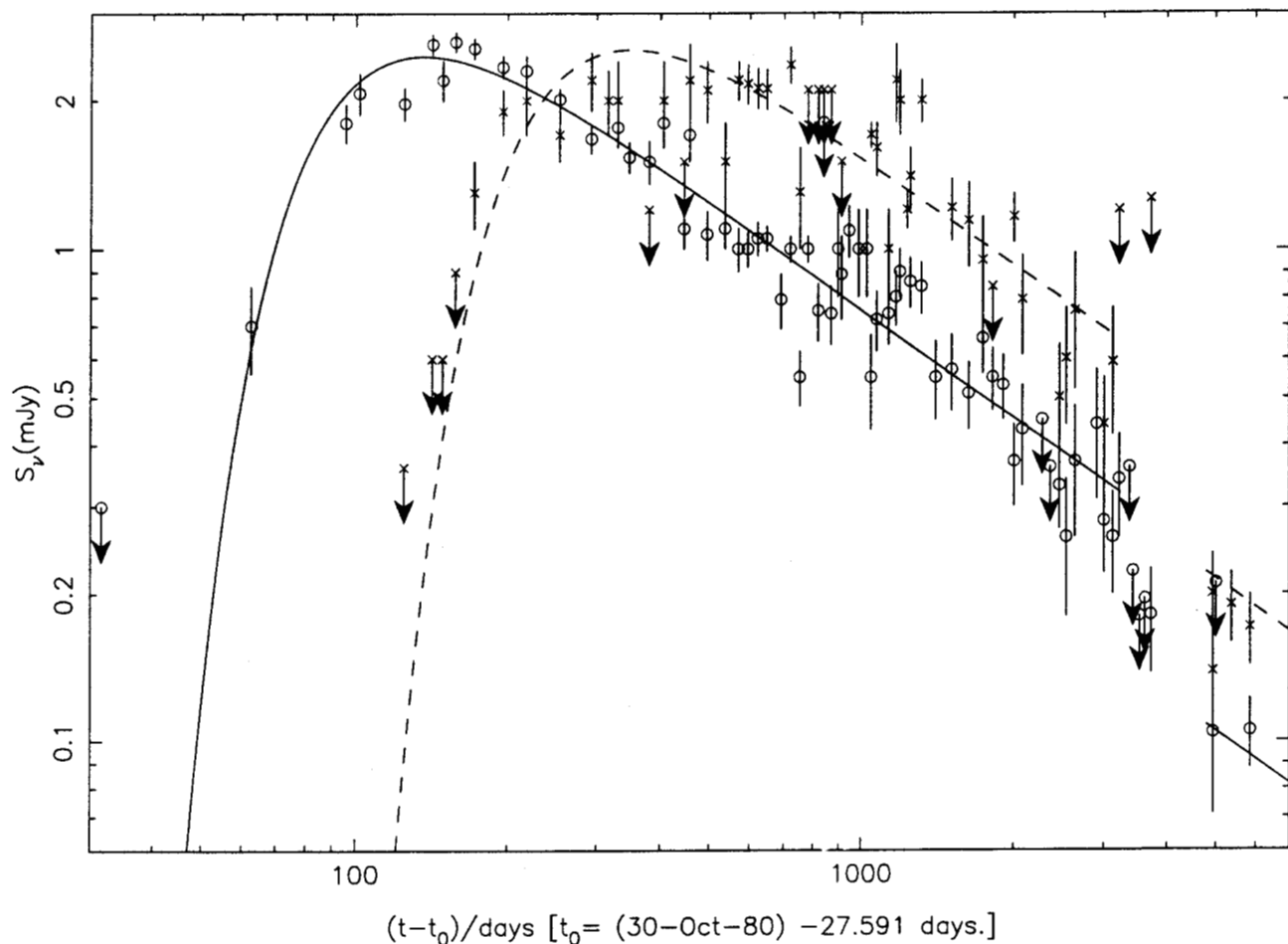


Fig. 2.— Radio light curves for SN 1980K in NGC 6946. The data at wavelengths 20 cm (*crosses*) and 6 cm (*open circles*) are shown together. The data represent 16 years of observation from 1980 November 3 through 1996 October 14, including new and revised observations presented in this paper and previous measurements, as well as new measurements. The *solid* and *dashed* curves up to day 3200 represent the best-fit model light curves at 6 and 20 cm, respectively. The curves after day 4900 are the extrapolation of the model appropriate up to day 3200 with the same decline rate  $\beta$  and same spectral index  $\alpha$ , but with a discontinuity of 55% introduced between day 3200 and day 4900.

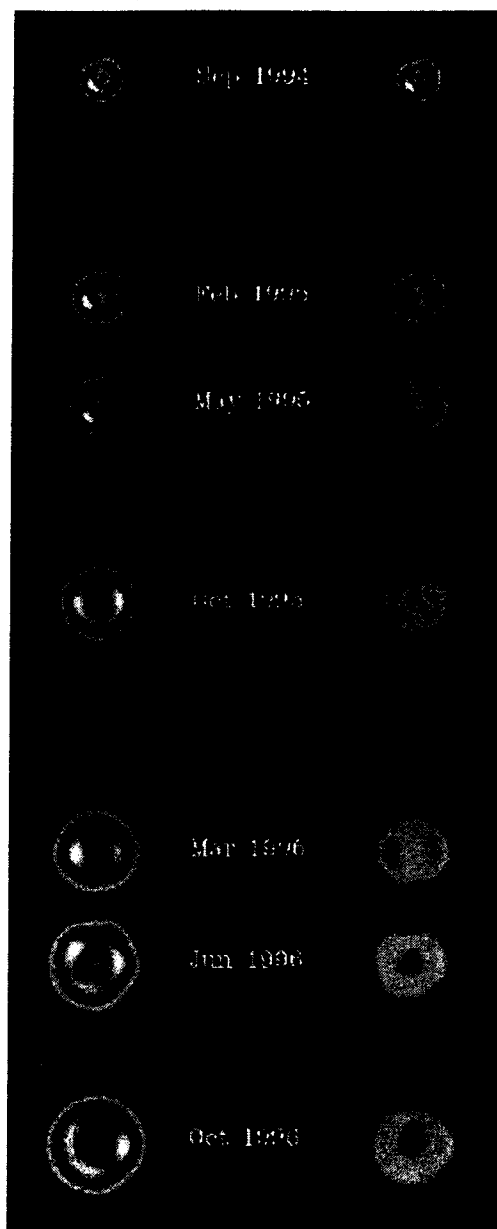


Fig. 3.— VLBI radio images of SN 1993J at 6 cm wavelength. Images on the left-hand side are normalized to the same peak brightness to emphasize structural changes. Images on the right-hand side are on a single brightness scale to illustrate the decrease in brightness with time.

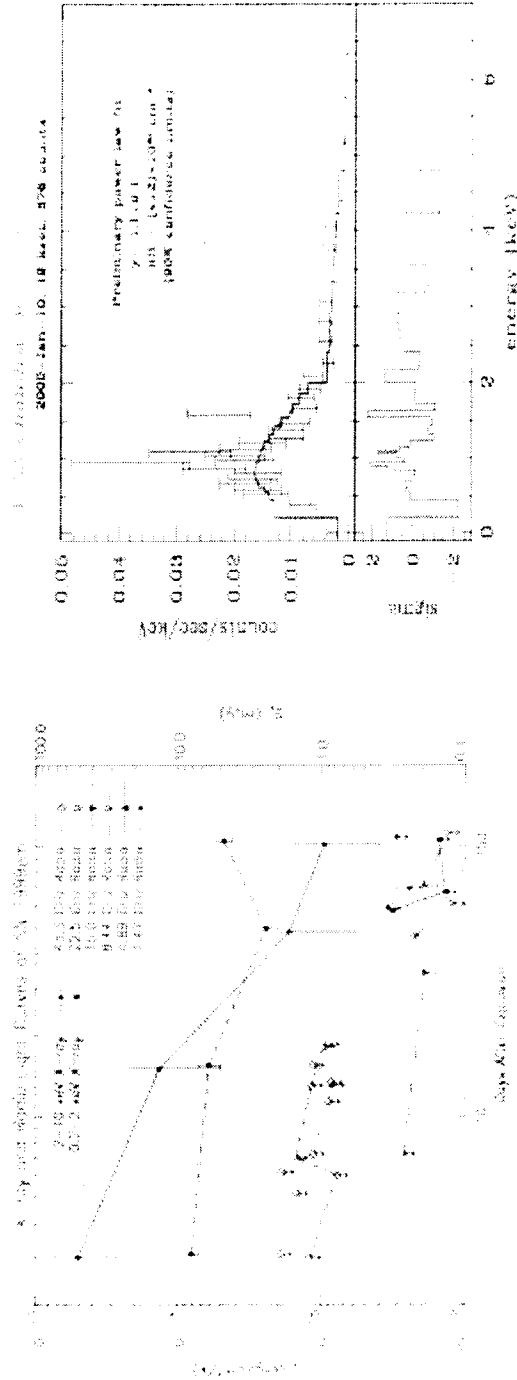


Fig. 4.— Left: light curves of SN 1999em. The X-rays continue to soften, and the radio data are mostly upper limits except for a handful of detections around X-ray minimum. Right: spectrum of SN 1998S with power law fit (solid line) and residuals (bottom plot). The possible emission features around 1 keV and 1.5 keV can be reproduced with thermal plasma models.

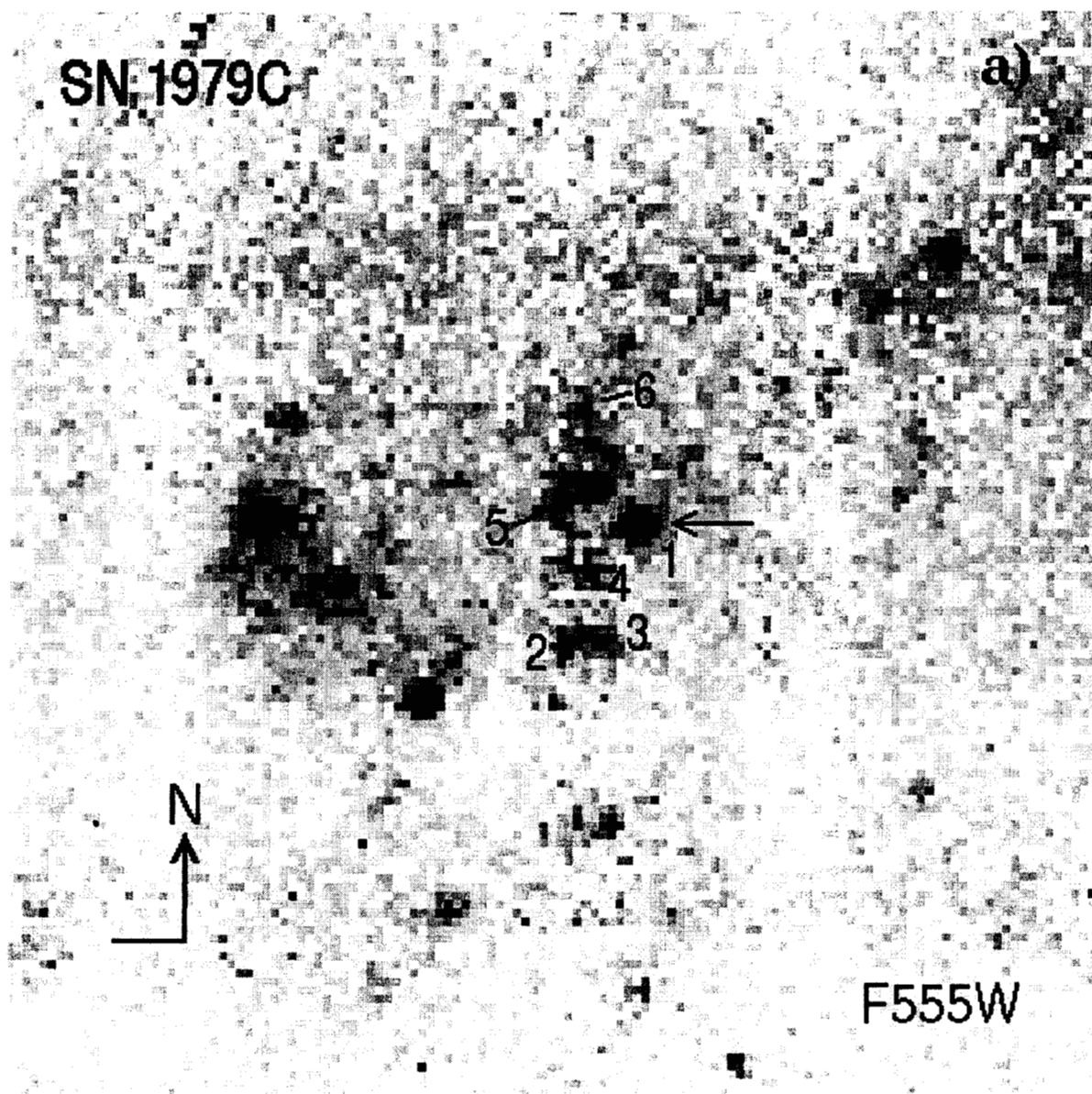


Fig. 5.— The environment of SN 1979C in NGC 4321 (M100), as seen on WFPC2 images obtained as part of GO 6584, in the F555W band. The arrow in each figure points to what is likely the SN itself. Orientation of the image is north up, east to the left.

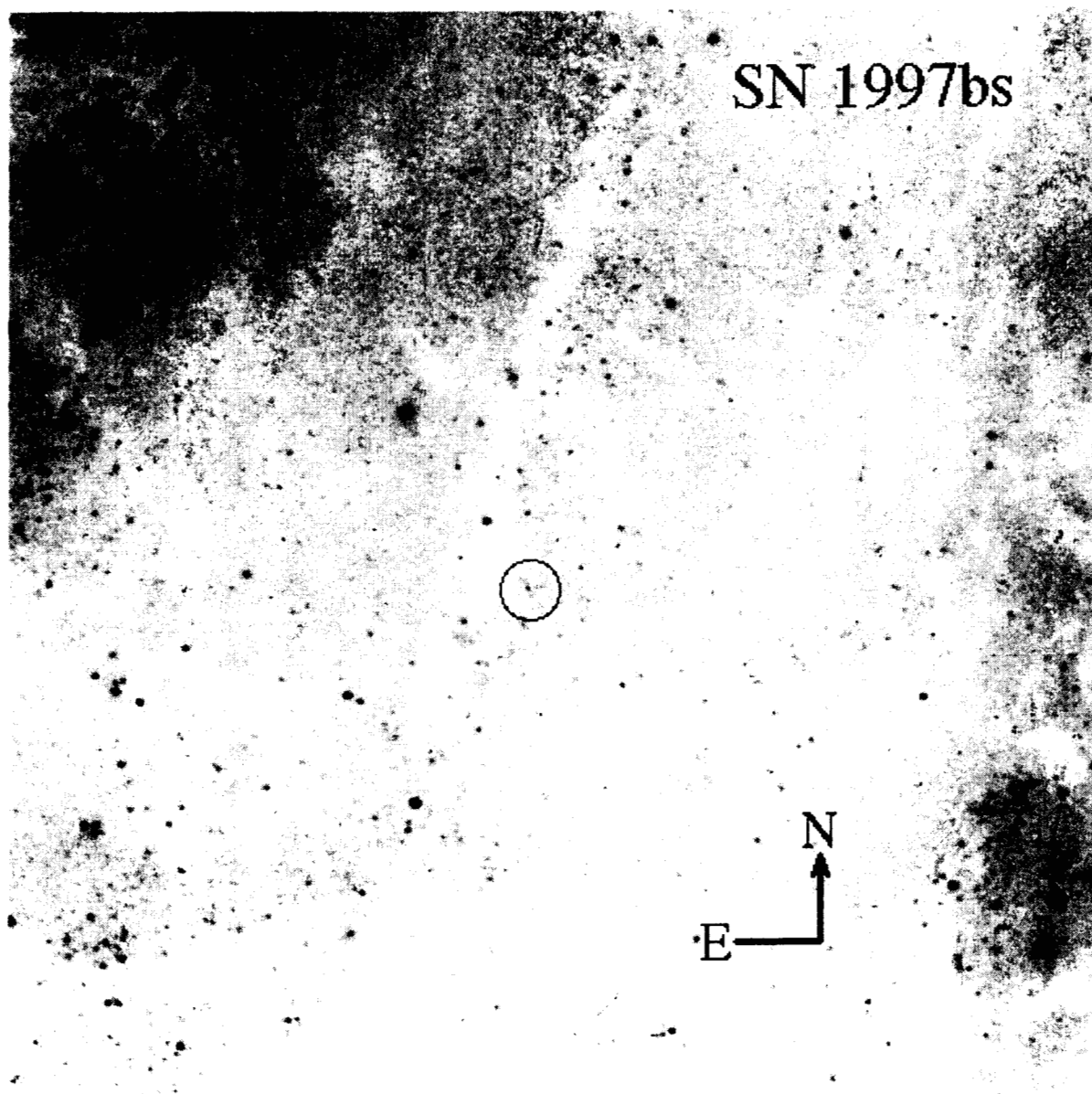


Fig. 7.— The environment of SN 1997bs in NGC 3627, as seen on a coadded F606W WFPC2 image. The SN position is within the  $1''$  radius error circle.